Visible Signatures of Hypersonic Reentry

Jeremy Teichman and Leon Hirsch

The Problem

Humans have observed glowing objects during atmospheric reentry for millennia, with some of the earliest known recordings of meteor showers dating to China in A.D. 36 (Imoto and Hasegawa 1958). The space age stimulated decades of scientific investigation of radiation during reentry of man-made objects (Maiden 1961). While state of the art observation is well documented, little quantitative analysis is available on the most rudimentary of capabilities—unaided human perception of these events. Our analysis explores whether, when, and where a reentry body will exhibit optical signatures visible to the unaided human eye.

Radiant Emissions

When an object moves through a gas faster than the speed of sound, it generates a shockwave. As gas passes through the shockwave, its pressure, density, and temperature suddenly rise. If the gas becomes sufficiently energetic, it will radiate electromagnetic energy with a wavelength and intensity related to its molecular content, density, and temperature. Aside from the gas, the reentry body's surface also heats up. The effects of surface heating and thermal conduction to internal structures influence applications such as hypersonic vehicles and reentry survivability (e.g., space shuttle tile damage). In our article, we restricted our analysis to the radiation from the impinging gas, which should be independent of the non-geometric qualities of the body.

The amount of radiation emitted depends upon the volume of the energized gas around the nose of the object. The integrated total visible spectrum radiant emission (luminous power) from the nose is approximately $\varphi = 0.1 J_S R^3_N$, where J_S is the volumetric luminous intensity at the stagnation point (scaling approximately as *Velocity*$^{8.5}$ *Density*$^{1.6}$) and R_N is the nose radius of curvature (Martin 1966). As an example, a body traveling at 6-km/s velocity and 30-km altitude, with a 50-cm nose radius of curvature will radiate 125 kW of visible light, which is the equivalent of about 60,000 100-W incandescent bulbs.

Atmospheric Optical Attenuation

Given the luminous power of the reentry body, how much luminous power reaches an observer on the ground?

> For many conditions, particularly at night, reentry bodies could be noticeable for hundreds of kilometers around the impact point for periods of time ranging from tens of seconds to minutes before impact.

The light radiated from the reentry body spreads, which reduces its flux in proportion to the distance squared, and attenuates exponentially through scattering and absorption in the atmosphere according to Lambert's Law (Brown 1965). The combined effect of these two principles is known as Allard's Law (Miller 1996),

$$E = \frac{\varphi}{4\pi D^2} e^{-\alpha_0 \frac{m}{m_0} H}, \qquad (3)$$

where E is the illuminance (incident visible light flux) at the observer, D is the distance separating the reentry body and observer, α_0 is the attenuation coefficient, m is the air mass traversed along the line of sight between the observer and the reentry body, m_0 is the total air mass in the atmosphere along a vertical column from sea level to space, and H is the scale-height of the atmosphere over which density decreases by a factor of e (approximately 6,700 m). When viewing through the atmosphere, the viewing elevation angle, θ, has a pronounced effect. The air mass traversed when viewing at the horizon is 38 times greater than looking straight up at zenith (Young 1989). We derived the following expression of the air mass traversed for a given elevation angle:

$$\frac{m}{m_0} = \sqrt{\frac{\pi R_E}{2H}} e^{\frac{R_E \sin^2 \theta}{2H}} \left(\mathrm{erf} \sqrt{\frac{z^2 + 2zR_E + R_E^2 \sin^2 \theta}{2HR_E}} - \mathrm{erf} \frac{\sqrt{R_E} \sin \theta}{\sqrt{2H}} \right) \quad (4)$$

where R_E is the radius of the earth and z is the altitude of the object.

With Equation (3) we calculate how much illuminance, or total visible light flux, would reach a ground observer. From the observer's perspective, the reentry body's brightness or luminance depends upon both the illuminance and the amount of sky occupied by the reentry body. In other words, a very bright but small light source can provide as much illumination as a dim but very large source. This principle is easily observed on a long stretch of a city street that has traffic lights visible for multiple blocks ahead. Farther lights appear smaller, but their brightness appears undiminished. When a source is sufficiently far away, it appears as a point source (i.e., the minimum resolvable size). Beyond this distance, the illuminance still decreases with distance, but the apparent size remains constant, which causes the apparent luminance to decrease with distance. Apparent luminance is calculated using apparent angular size:

$$L = \frac{E}{\Omega_{Apparent}}, \qquad (5)$$

where $\Omega_{Apparent}$ is the light source's size from the perspective of the observer. This is either the solid angle subtended or the minimum resolvable solid angle, whichever is larger.

Limits of Human Perception

The most basic determinant of whether an object is discernible by the unaided human eye is the object's contrast with the background. Contrast, C, is defined as the excess brightness of the object relative to the background luminance, L_0:

$$C = \frac{L - L_0}{L_0}. \qquad (6)$$

An object brighter than the background presents positive contrast, while an object darker than the background presents negative contrast. The absolute value of

contrast determines visibility so negative and positive contrasts of the same magnitude contribute equally to visibility (Gordon 1964). Positive contrast has no limit, whereas negative contrast cannot exceed a value of -1. The size of an object also contributes to its visibility, with larger objects being more visible. Below a critical angular size, objects appear as point sources, and size does not contribute directly to visibility. The third variable contributing to human visibility thresholds is ambient light level. Human eyes require greater contrast at lower ambient light levels. While the eye can discern a contrast of about 0.4 in daylight, it requires a contrast of about 710 in starlight. The critical angular size below which objects appear as point sources also grows with lower ambient light levels, ranging, from about 0.2 mrad in daylight to 2 mrad in starlight. Blackwell quantified the threshold contrast level as a function of object size and ambient light level (Blackwell 1946).

Noticeability

The examples above pertain to what humans will detect with careful study of the sky. This was not our motivation. Rather, our analysis sought to quantify what a casual observer would notice without cueing, foreknowledge, or viewing the sky at object's precise location. This phenomenon is termed "attention capture," (i.e., what people will notice). However, the literature's findings on this subject vary and depend upon many confounding factors such as the subject's task and state of mind, the dynamics and colors of the target, or background. (Simons 2001).

As a more widely accepted surrogate for noticeability under different conditions, our analyses adopted the Federal Aviation Administration (FAA) regulations for obstruction lighting on tall structures (to alert pilots of their presence and avoid collisions). For example, the FAA mandates obstruction lights of 100,000 candela luminous intensity to provide daytime visibility (noticeability) at 4.3 km on a day with 4.8-km meteorological visibility (U.S. Department of Transportation, Federal Aviation Administration 2007).

Applying Allard's Law with assumptions for background illumination and size of the light, we estimate a contrast value of 39 for FAA daytime obstruction lighting, compared to a threshold of 0.37; which leads to a contrast ratio of approximately 100x. The same can be done for the nighttime requirements to yield a contrast ratio of 200–400x. In both cases, the FAA lighting requirement is on the order of a few hundred times the minimum contrast threshold for detectability. We adopted a 400x threshold contrast level as the standard for high noticeability.

Results

Figure 1 displays noticeability of a reentry body at an instant in time. For a reentry body with a nose/leading-edge radius of curvature of 0.5 m, a velocity of 7 km/s, and an altitude of 50 km, the figure presents contrast level normalized to the threshold contrast level. A value of 1 indicates marginal detectability, and a value of 400 indicates noticeability equivalent to FAA standards for obstruction lights. Both of these levels
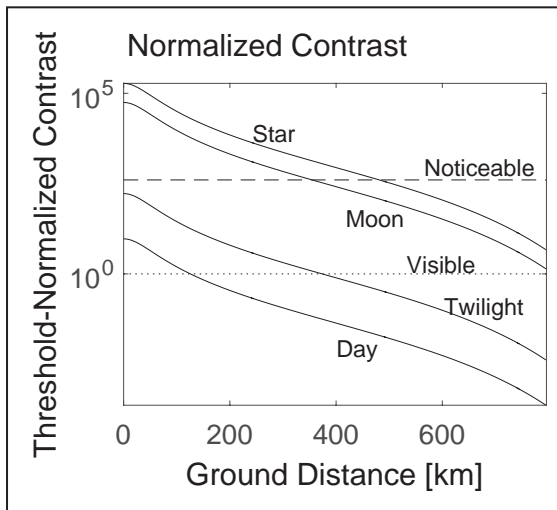
Figure 1. Metrics for Visibility

are indicated on the plot. The value of the metric is plotted over the ground distance of an observer from nadir below the reentry body. Curves are shown for four different ambient light adaptation levels: dark cloudless (moonless) night (labeled 'Star'), full moon night (labeled 'Moon'), zenith brightness at sunset (labeled 'Twilight'), and zenith brightness at 10:30 a.m. (labeled 'Day'), which represents a sun elevation angle of 60° (e.g., 10:30 a.m. in Washington, D.C., on July 21, 2009).

According to Figure 1, the reentry body would be noticeable at night at distances of nearly 500 km from nadir, even on a full moon night. During the day, however, the same reentry body would be detectable but not noticeable to the 400x threshold standard, even from directly below.

We next consider duration of noticeability for reentry bodies with different amounts of lift—ranging from purely ballistic (no lift) to gliding with a lift-to-drag ratio of 2. For each case, the reentry body possessed a

nose radius of curvature of 0.5 m, a drag coefficient of 0.3, a diameter of 1 m, a mass of 1,000 kg, and initial velocity of 7 km/s. Simulations began at an altitude of 150 km (a point where atmospheric density becomes sufficiently high to generate visible signatures).

For the purely ballistic case, Figure 2 depicts periods of noticeability for different ambient lighting conditions. The center of the figure, marked zero distance downrange and crossrange denotes the point of impact. Ballistic reentry occurs quickly. With its brief time in the atmosphere confined to region about the point of impact, duration of noticeability is relatively brief, 20 seconds or less for all lighting conditions.

For the gliding case of Figure 3, the reentry body aerodynamically skips across the atmosphere multiple times. Eight pull-up cycles result in noticeability over 8,000 km up-range from the point of impact. Under daylight conditions, there is little opportunity to view the object at any point along the trajectory. Under dimmer lighting conditions, the object is visible for extended periods of time (over 2 minutes) uprange. Once the reentry body is within a few hundred kilometers from the point of impact, it has lost enough energy that it is no longer visible under any lighting conditions. Note, however, that due to the large ranges considered for this trajectory, lighting conditions would vary over this span of distances; the ground track of the 8,000 km aerodynamic portion spans about five time zones. In short, it could be nighttime at the first point of entry and twilight at the point of impact.
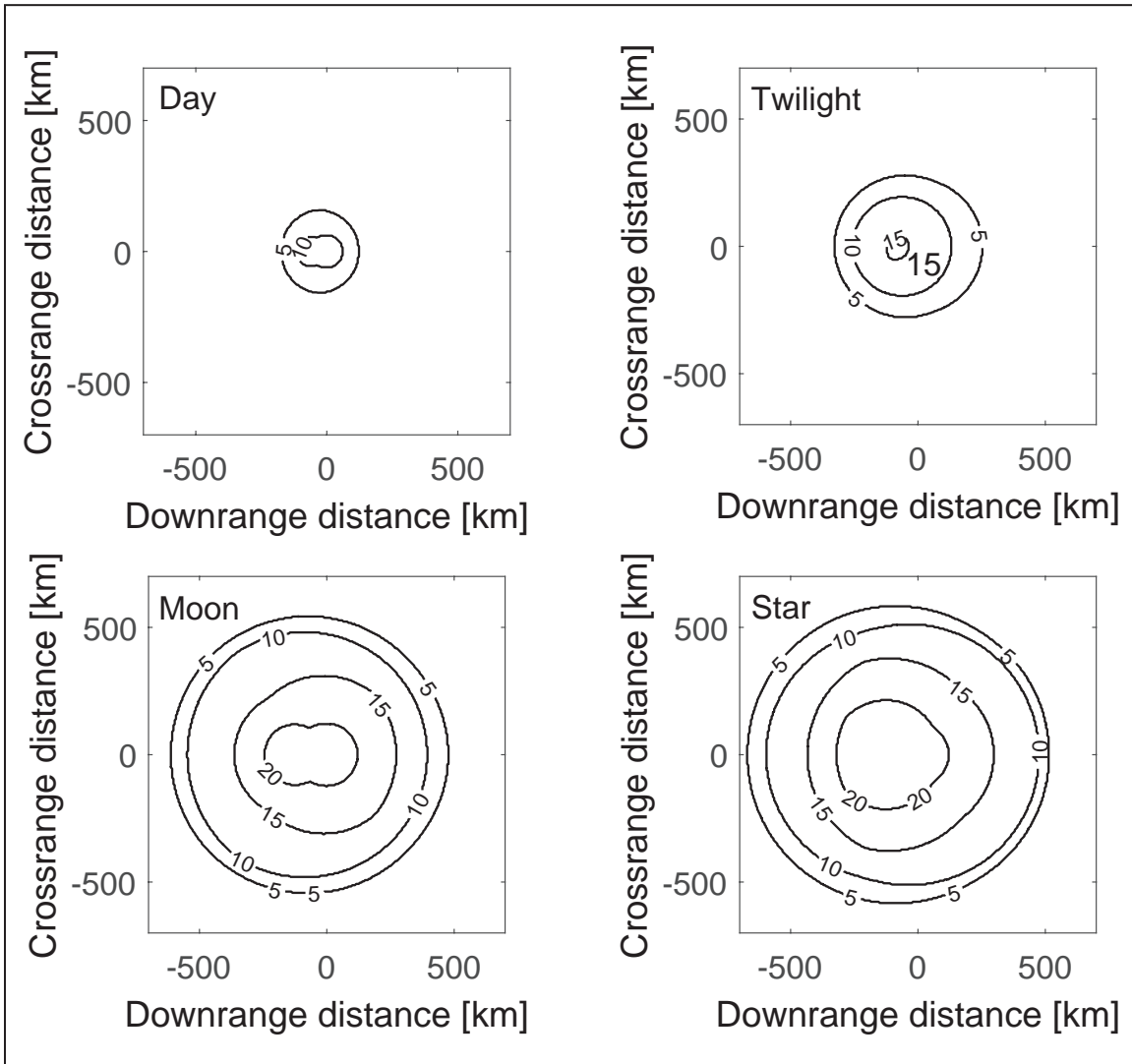
Figure 2. Duration of Noticeability [seconds], L/D = 0

Conclusion

For a given reentry body, we estimate the noticeability and visibility regions using criteria extrapolated from FAA lighting visibility requirements. For many conditions, particularly at night, reentry bodies could be noticeable for hundreds of kilometers around the impact point for periods of time ranging from tens of seconds to minutes before impact. Purely ballistic reentry bodies of the scale in the examples shown would be noticeable for hundreds of kilometers at night over regions including the impact point but for less than a minute prior to impact. Strongly lifting reentry bodies could be visible thousands of kilometers uprange of impact for over a minute as they skip off the denser atmosphere, but they would slow sufficiently with successive skips that, by the time they come over the impact point's horizon, they would no longer be noticeable.
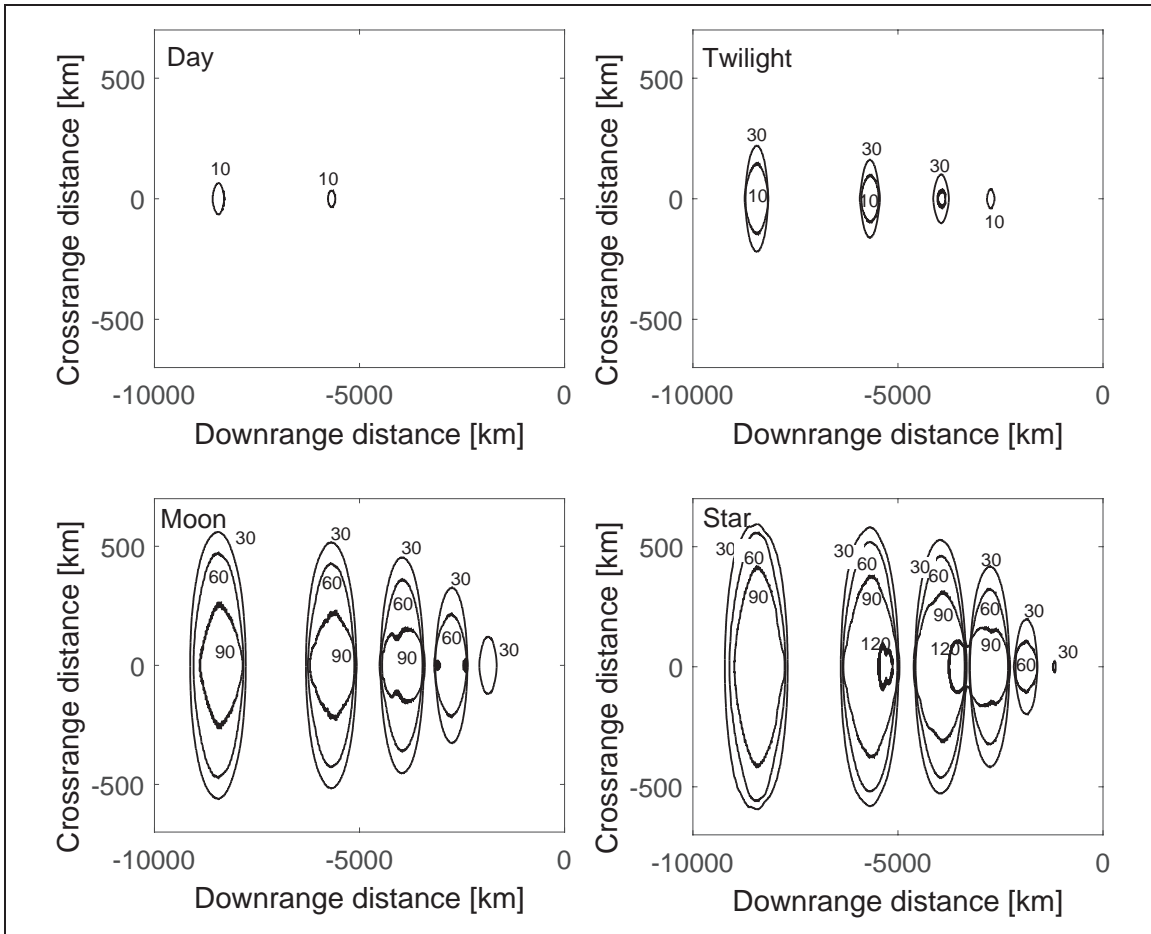
Figure 3. Duration of Noticeability [seconds], L/D = 2

Dr. Teichman is a Research Staff Member in IDA's Science and Technology Division. He holds a Doctor of Philosophy in mechanical engineering from the Massachusetts Institute of Technology.

Dr. Hirsch is a Research Staff Member in IDA's Science and Technology Division. He holds a Doctor of Philosophy in bioengineering from Rice University.
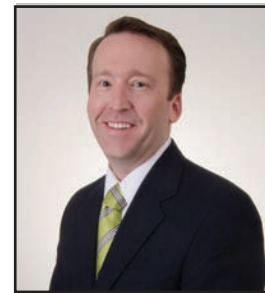
The original article was published in the *Journal of Spacecraft and Rockets,* April 2014.

"Visible Signatures of Hypersonic Reentry"

http://arc.aiaa.org/doi/abs/10.2514/1.A32667

References

Blackwell, H. R. "Contrast Thresholds of the Human Eye." *Journal of the Optical Society of America* 36, no. 11 (1946).

Brown, Earle B. *Modern Optics*. New York: Reinhold Publishing Corp., 1965.

Crawford, D. L. "Photometry: Terminology and Units in the Lighting and Astronomical Sciences." *The Observatory* 117 (1997): 14-18.

Dixon, Michael, Roy Rasmussen, and Scott Landolt. *Short-Term Forecasting of Airport Surface Visibility Using Radar and ASOS*. Boulder, CO: National Center for Atmospheric Research, n.d.

Gordon, J. "Visibility: Optical Properties of Objects and Backgrounds." *Applied Optics* 3, no. 5 (1964).

Hidalgo, H., and R.W. Detra. "Generalized Heat Transfer Formulas and Graphs for Nose Cone Reentry into the Atmosphere." *Journal of the American Rocket Society* 31 (1961): 318.

Imoto, S., and I. Hasegawa. "Historical Records of Meteor Showers in China, Korea, and Japan." *Smithsonian Contribution to Astrophysics* 2, no. 6 (1958): 131.

Koschmieder, Harald. "Theorie der horizontalen Sichtweite (The theory of horizontal visual range)." *Beitrage zur physik der freien Atmosphare* 12 (1924): 33-55.

Maiden, C. J. *Aerophysical Studies at Hypersonic Velocities in Free Flight Ranges*. Vols. 3-4, in *Advances in Aeronautical Sciences*. Oxford: Pergamon Press, Ltd., 1961.

Martin, John J. *Atmospheric* Reentry. New Jersey: Prentice-Hall, 1966.

Miller, Edward Friedman and John Lester. *Photonics rules of thumb: optics, electro-optics, fiber optics, and lasers*. McGraw-Hill, 1996.

Mills, A. F. *Heat and Mass Transfer*. Boston: Richard D. Irwin, Inc., 1995.

National Advisory Committee for Aeronautics. "Report 1135: Equations, Tables, and Charts for Compressible Flow." 1953.

Ridpath, Ian, ed. *Norton's 2000.0* Star Atlas and Reference Handbook. 18. Essex: Longman Scientific and Technical, 1989.

Scolnik, L. Dunkelman and R. "Solar Spectral Irradiance and Vertical Atmospheric Attenuation in the Visible and Ultraviolet." *Journal of the Optical Society of America* 49, no. 4 (1959).

Simons, S. B. Most and D. J. "Attention Capture, Orienting, and Awareness." In *Attraction, Distraction, and Action: Multiple Perspectives on Attentional Capture*, edited by C. L. Folk and B. S. Gibson. Amsterdam: Elsevier Science B.V., 2001.

U.S. Department of Transportation, Federal Aviation Administration. "Obstruction Marking and Lighting." *Advisory Circular AC 70/7460-1K,* February 2007: Appendix 2.

Young, F. Kasten and A. T. "Revised optical air mass tables and approximation formula." *Applied Optics* 28, no. 22 (1989).

Zombeck, *Martin. Handbook of Space Astronomy and Astrophysics*. Cambridge, UK: Cambridge University Press, 1990.